

Response to Referee #1

In the current manuscript, Li et al. have used the very high temporal and spatial resolution of the ground-based OH and OI airglow network to look at the upper atmosphere response to the HTHH (Hunga Tonga-Hunga Ha'apai) Volcanic Eruption occurred in 2022, which has been an active and important research topic after the eruption. OH airglow (see Figure 1) measurements have detected five group atmospheric waves in the ground-based airglow network (the first wave packet is observed after 8 hours). Then they have obtained the phase speed and amplitude over 10 hours period (see Figure 2). The wave front can be also observed by OI airglow at higher altitude ~250 km. The authors also noticed that short period of sudden surface pressure changes over Xinglong station, which were caused by the pressure disturbances that spread out in the form of Lamb waves due to HTHH eruption. The authors also carried out tsunami model simulations using two sources (one is the localized source, termed TITVE, the other considers the atmospheric pressure changes, termed as TIAPW) to investigate the propagating speed to China due to different tsunami sources used in the model. Then they discussed the air-sea interactive process on the upper atmospheric responses to HTHH eruption. They also did some related important diagnosis about the vertical wavelength and ray path of the waves etc. Finally they provided a nice figure describing the dynamic coupling process between air and sea via acoustic gravity waves. Overall, the paper has a clear structure and the motivation is clear. This study is important and interesting.

However, sometimes it is unclear to me because the figures are not clear enough or some descriptions/explanations are vague (see the detailed comments below). It requires some clarification.

Thank you very much for your thoughtful and constructive comments concerning our manuscript entitled "Upper Atmosphere Responses to the 2022 Hunga Tonga-Hunga Ha'apai Volcanic Eruption via Acoustic-Gravity Waves and Air-Sea Interaction". Those comments are all valuable and very helpful for revising and improving our paper, as well as the important guiding significance to our researches. We have studied comments carefully and have made corrections which we hope meet with approval. The detailed point-by-point responses are given below.

I have two major concerns:

One is the tsunami model simulations by assuming two sources. I can not see any information about the model. Is that a global model or regional model? What are the necessary/important input required to model tsunami? How is the model performances to represent the tsunami due to HTHH volcanic eruption?

Response:

Thank you very much for your comments. We have provided a more detailed description of the tsunami model simulations

2.2 Tsunami simulation model

Tonga submarine volcano erupted on 15 January 2022, and generated tsunamis that were detected around the globe, affected particularly the Pacific region. In this study, two types of tsunamis were simulated, conventional tsunami simulations and atmospheric pressure wave-induced tsunami simulations. The linear-shallow water equations in the spherical coordinate system are used to simulate the tsunamis from the localized source and atmospheric pressure wave. The continuity equation of a linear shallow water wave model in spherical coordinates is:

$$\frac{\partial \eta}{\partial t} + \frac{1}{R \sin \theta} \left[\frac{\partial(ud)}{\partial \varphi} + \sin \theta \frac{\partial(vd)}{\partial \theta} \right] = 0 \quad (1)$$

where η is free surface elevation (m), d is the water depth (m), R is the Earth's radius (6371,000 m), φ is longitude, θ is colatitude.

While the momentum equations of the linear shallow water wave model are:

$$\frac{\partial u}{\partial t} + \frac{1}{R \sin \theta} \left[g \frac{\partial \eta}{\partial \varphi} + \frac{1}{\rho} \frac{\partial p}{\partial \varphi} \right] + fv = 0 \quad (2)$$

$$\frac{\partial v}{\partial t} + \frac{1}{R} \left[g \frac{\partial \eta}{\partial \theta} + \frac{1}{\rho} \frac{\partial p}{\partial \theta} \right] - fu = 0 \quad (3)$$

where, u is the velocity along the lines of longitude (m/s), v is the velocity along the lines of latitude, g is the gravitational acceleration (9.81 m/s²), p is the atmospheric pressure (Pa), ρ is the sea water density (1026 kg/m³), f is the Coriolis coefficient. For the atmospheric pressure wave-induced tsunami simulation, the moving change pressure terms as an input to tsunami simulation momentum equation. The atmospheric pressure wave model is based on the Equation (1) in Gusman et al. (2022).

For the tsunami simulations from a localized source, a B-spline function (Koketsu and Higashi, 1992) below is used to represent the circular water uplift source at the volcano:

$$f(x, y) = \sum_{i=0}^3 \sum_{j=0}^3 c_{k+i, l+j} B_{4-i} \left(\frac{x-x_k}{h} \right) B_{4-j} \left(\frac{y-y_l}{h} \right) \quad (4)$$

where

$$B_i(r) = \begin{cases} r^3/6, & i = 1 \\ (-3r^3 + 3r^2 + 3r + 1)/6, & i = 2 \\ (3r^3 - 6r^2 + 4)/6, & i = 3 \\ (-r^3 + 3r^2 - 3r + 1)/6, & i = 4 \end{cases} \quad (5)$$

x_k and x_l stand for the coordinates of the knots along the x and y axes, h is the characteristic diameter of water uplift, r is the great-circle distance from the volcano eruption center, $c_{1,1} = 1$ and the other $c_{k+i,l+j} = 0$. In this study, the modelling domain covers the Pacific Ocean and some parts of Indian Ocean and the Caribbean with a grid size of 5 arc-min. For detailed tsunami simulation algorithms, please refer to Gusman et al. (2022).

References

Gusman, A.R., Roger, J., Noble, C. et al. The 2022 Hunga Tonga-Hunga Ha'apai Volcano Air-Wave Generated Tsunami, *Pure and Applied Geophysics*, 179, 3511–3525, <https://doi.org/10.1007/s00024-022-03154-1>, 2022.

Koketsu K. and Higashi S.: Three-dimensional topography of the sediment/basement interface in the Tokyo Metropolitan area, Central Japan, *Bull. seism. Soc. Am.*, 82, 2328-2349, <https://doi.org/10.1785/BSSA0820062328>, 1992.

The other is about the inconsistent use of meteorological data product when the authors did some diagnosis (for example vertical wave numbers, lines 120-125). The authors use temperature profiles from SABER (20-100km) and the wind from both ERA5 and HWM-14. I know ERA5 is only up to 85 km and the authors would like the profile of vertical wave number up to 100 km. Which altitude range use ERA5, then HWM-14. How realistic is the HWM-14 modelled wind changes (since this model is an empirical model which only uses geomagnetic Ap index) due to the HTHH volcanic eruption? What will be the difference when you use both ERA5 wind and temperature profiles below some certain altitude compared with the current result?

Response:

Thank you for your criticism and comments. Yes, you are right. The HWM wind field is an empirical model wind field that can only reflect a long-term trend, which is not suitable for event research. Therefore, we use meteor radar wind fields to replace the HWM wind fields. The ERA-5 wind field is used in the areas below the mesopause region. Here, we use a total of 137 layers of ERA-5 wind field, with heights from the ground to 80 km. The upper boundary area may have errors due to sponge layer effects.

The height range of ERA-5 wind field used is from 0 to 75 km, and above 75 km, meteor radar wind field is used. We have reconfirmed the location of wave sources in ray tracing analysis using new wind field data.

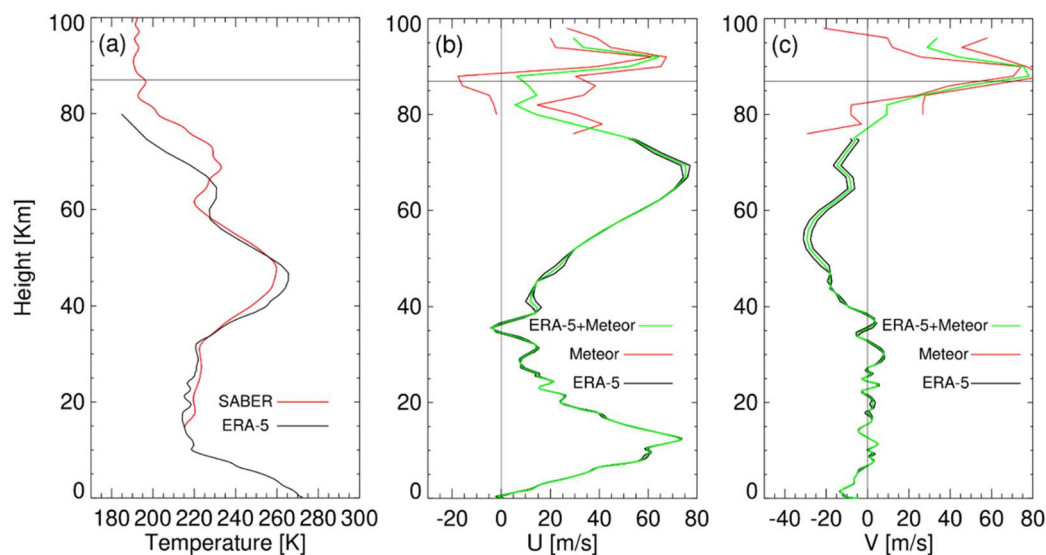


Figure 10 The background field used for ray tracing analysis for the TIAPW event (a) Saber temperature (red) comes from the average temperature of ascending track #1 and descending track #1 in Fig. 9, and ERA-5 temperature (black) comes from the average of 15:00 UT and 16:00 UT. (b) Meteor zonal wind field (red) and ERA-5 zonal wind field (black). (c) Meteor meridional wind field (red) and ERA-5 meridional wind field (black). The two red and black lines in (b) and (c) are respectively from 15:00 UT and 16:00 UT. The green lines represent the average of two lines. Meteor radar wind field is from Beijing station.

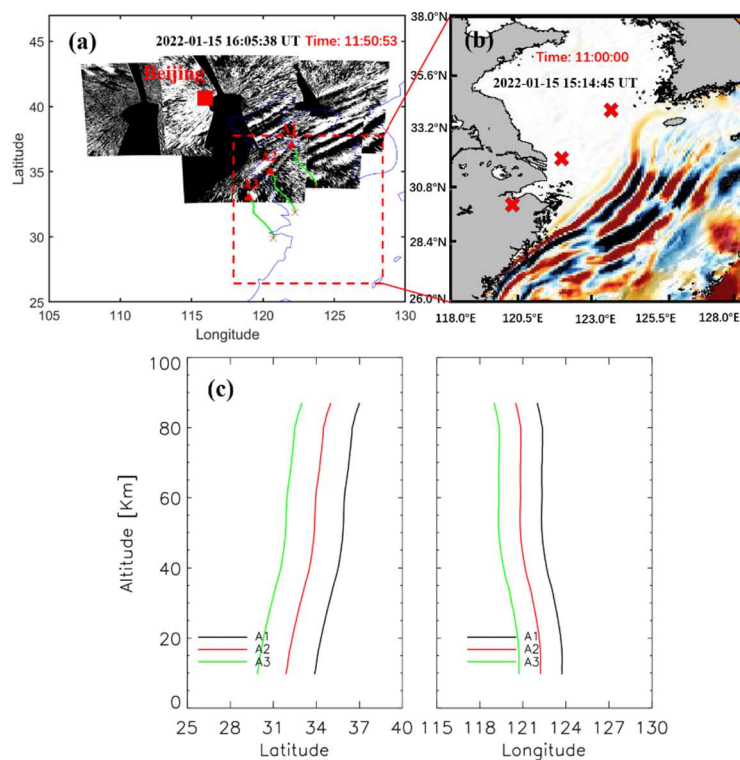


Figure 11 (a) Backward ray tracing results of the wave packet #3 observed by the OH airglow network. The red triangles and red crosses represent the trace start and termination points, respectively. (b) Simulated tsunamis induced by the atmospheric pressure wave (TIAPW) corresponding to the dotted rectangular area in (a). (c) Ray paths of the wave starting from the seven sampling points in (a).

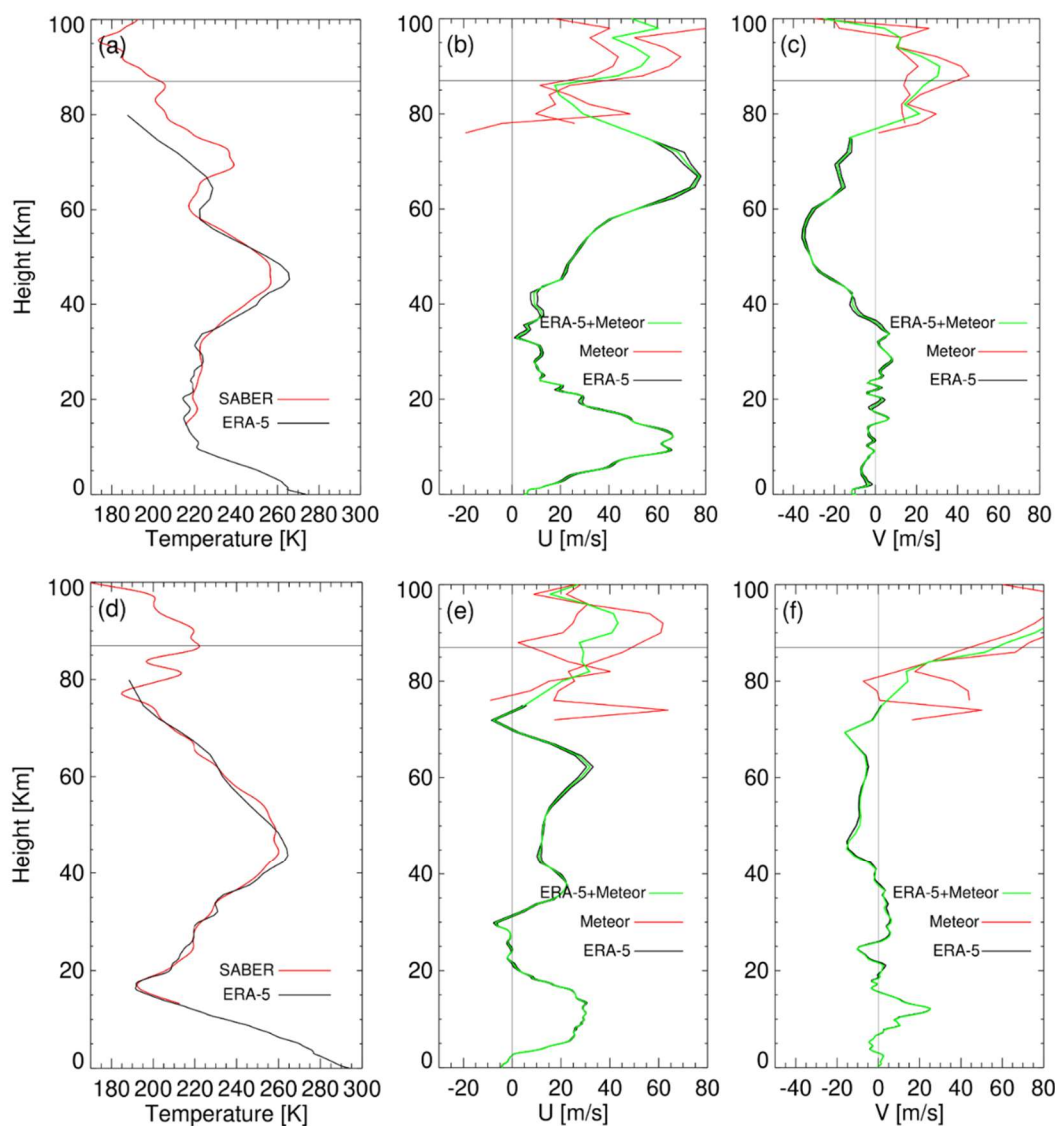


Figure 12 Similar for Figure 10, but for ray tracing analysis for the TITVE events. The SABER temperature field in (a) comes from ascending track #1 (21:17:50 UT, 21:18:33UT, 21:19:43 UT, and 21:20:43 UT) in Fig. 9, and the meteor radar wind fields in (b) and (c) come from Beijing station. The SABER temperature field in (d) is from ascending track #1 (21:12:51UT, 21:14:01 UT, and 21:14:44 UT) in Fig. 9, and the meteor radar wind fields in (e) and (f) are from Ledong station.

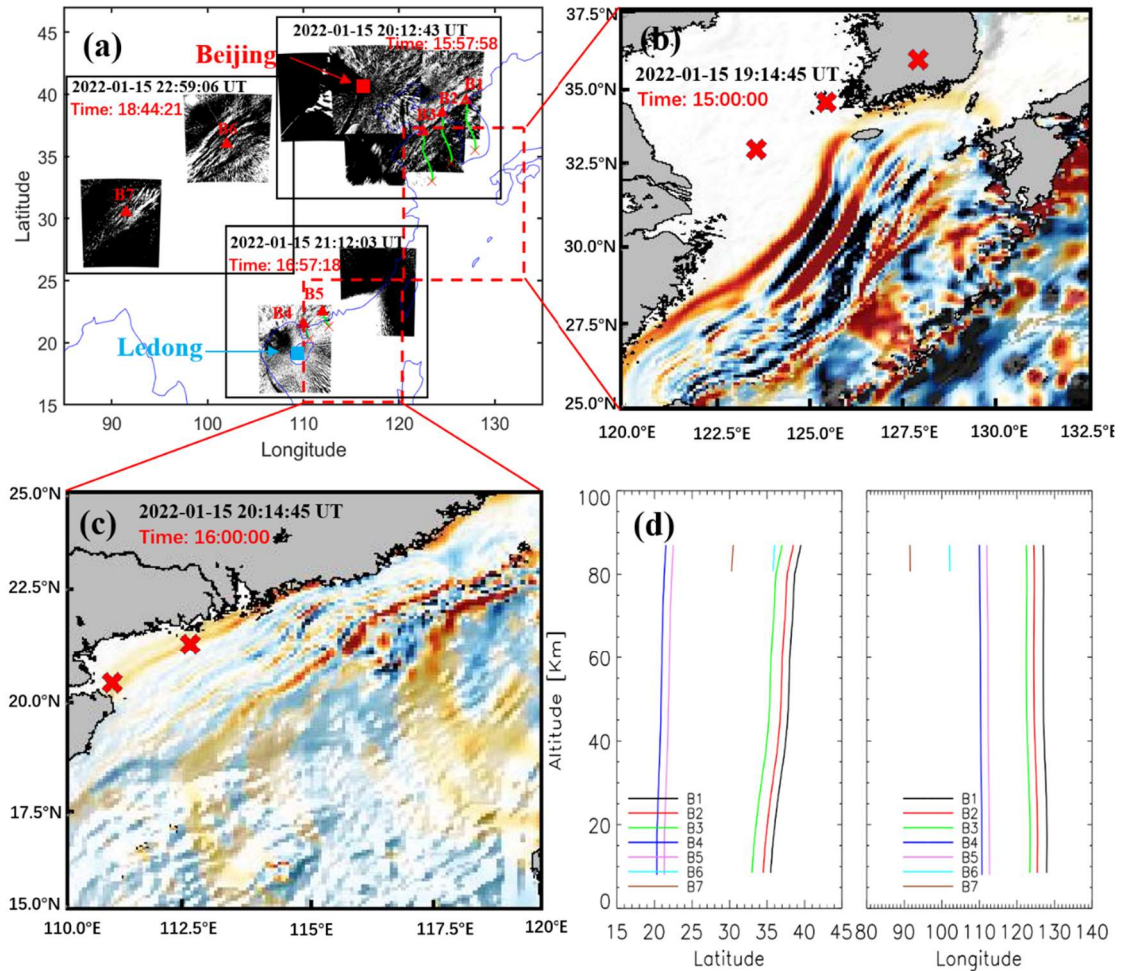


Figure 13 (a) Backward ray tracing results of the fourth and five group GWs observed by the OH airglow network. The red triangles and red crosses represent the trace start and termination points, respectively. (b) and (c) Simulated tsunami directly induced by the Tonga volcano eruption (TITVE) corresponding to the dotted rectangular area in (a). (c) Ray paths of the wave starting from the seven sampling points in (a).

Following your suggestion, taking the TIAPW event as an example, we compared the differences in ray tracing results between Sabber temperature and ERA-5 temperature. Figure S1 (below) shows the deviation of ray tracing trajectories obtained from two different temperatures. From the ray tracing trajectory, there is no significant deviation between the two (with a maximum error of $\pm 0.32^\circ$), and some areas almost overlap.

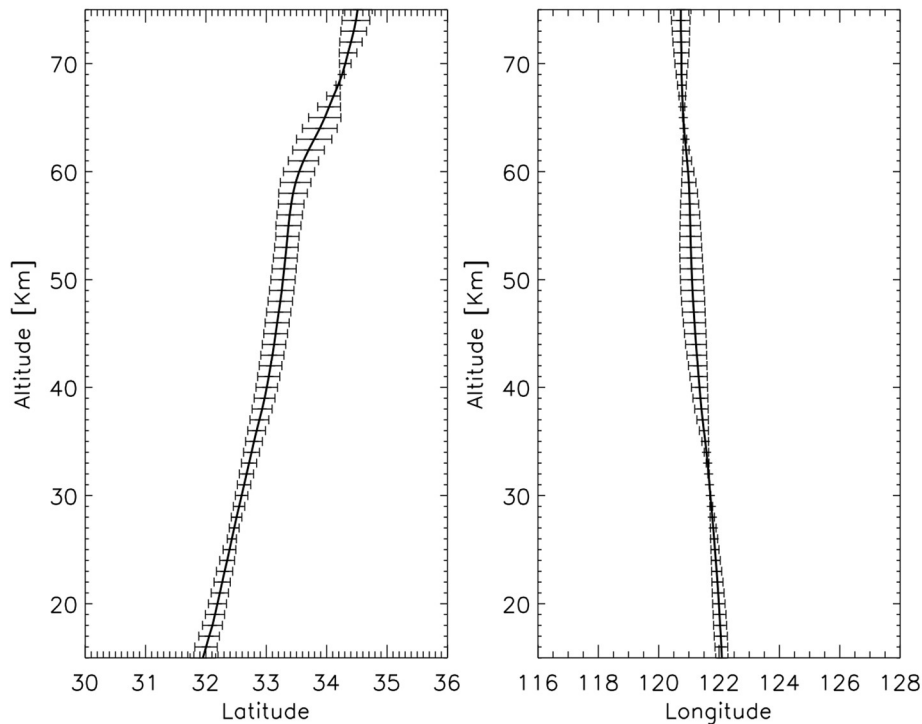


Figure S1 Deviation of ray tracing trajectories obtained from two different temperatures

In the Introduction, the authors have introduced HTHH volcanic eruption triggered broad spectrum atmospheric disturbances including different waves (Lines 41-44), but the second paragraph mainly focuses on Lamb waves. Why are other waves ignored?

Response:

Thank you for your suggestion.

The discussions of other waves are given below

Acoustic-gravity waves (AGWs) are mechanical waves in compressible fluids in a gravity field (Gossard and Hooke, 1975). If the frequencies are much larger than the buoyancy frequency, AGWs tend towards acoustic wave mode, and when the frequency is much smaller than the buoyancy frequency, the fluid can be considered incompressible, and the AGWs tend towards internal GWs mode. The term “acoustic-gravity waves” is usually used when restoring forces due to both gravity and compressibility are important. AGWs are known to play a significant role in the coupling between the atmosphere and the ocean (Donn and Balachandran, 1981; Harkrider and Press, 1967; Press and Harkrider, 1962). Atmospheric pressure waves are mechanical waves that are related to the density of the atmosphere. Compression and expansion are the high-pressure and low-pressure regions of motion in a medium.

Specified comments:

- Line 54, it reads weird “from GNSS TEC analysis”. Better to change what “analysis” method used based on “GNSS TEC”. The acronym “GNSS TEC” should be described when they first appear in the text.

Response:

Thank you very much for your comment. We re-described this sentence as: "Li et al. (2023) identified Lamb wave L1 mode using phase-leveling amplitude technology based on global navigation satellite system (GNSS)- total electron content (TEC)." in the revised manuscript.

- Lines 58-60. Can you provide some explanation about the “atmospheric pressure wave”?

Response:

Atmospheric pressure waves are mechanical waves that are related to the density of the atmosphere. Compression and expansion are the high-pressure and low-pressure regions of motion in a medium.

- Line 60, AGWs is defined in the Abstract for the first time but not in the main text. Better to define it here.

Response:

Thank you very much for your comment.

We define AGWs here:

Acoustic-gravity waves (AGWs) are mechanical waves in compressible fluids in a gravity field (Gossard and Hooke, 1975).

- Line 61, please delete “the height of”.

Response:

“the height of” is removed from the revised manuscript.

- Line 64, the authors need to make clear “that arrived before the tsunami”, for example when/where Tsunami occurred, how many hours earlier etc.

Response:

Thank you very much for your comment. We re-described this sentence as: "Using the red line airglow imager, Makela et al. (2011) detected airglow disturbance in Hawaii that arrived 1hr earlier of the tsunami generated by the 11 March 2011 Tohoku earthquake." in the revised manuscript.

- Line 65. Again, it is very vague “sea wave and GW almost simultaneously in Chile”. I guess the authors still talk about tsunami, but should make it clear if this is the same Tsunami as mentioned in Line 64.

Response:

Thank you very much for your comment. We re-described this sentence as: "Smith et al. (2015) observed tsunamis and GW almost simultaneously in Chile." in the revised manuscript.

- Line 66, though readers know 3D is three dimensional, better to add this after 3D.

Response:

“three dimensional” is added to the revised manuscript like this “three dimensional (3D)”.

- Lines 69-70, I am confused with “AGWs on the mesopause airglow radiation”.

Response:

Thank you very much for your comment. We re-described this sentence as: "Inchin et al. (2022) performed the numerical simulations of mesopause airglow radiation fluctuations induced by tsunami-generated AGWs” in the revised manuscript.

- Line 73. What is “convention tsunami”?

Response:

Conventional tsunamis are typically generated by localized sea surface displacements caused by sources such as earthquakes and volcanoes.

- Line 75, What is “this typical type tsunami”?

Response:

This typical type tsunami is convention tsunami.

- Lines 58-59, 77-78. Again, It is not clear why “tsunamis induced by the atmospheric pressure wave (TIAPW)” is more important than “tsunamis directly induced by the 2022 Tonga volcano eruption (TITVE)”.

Response:

Thank you very much for your comment.

We are very sorry for the confusion caused by our description. Both types of tsunamis are very important.

“Another significant mechanism that occurred was the atmospheric pressure wave that excited the tsunamis.” is changed to “Another tsunami is induced by the atmospheric pressure wave (TIAPW).”

The following description is removed from the manuscript

“Neither has AGWs originate from tsunamis induced by the atmospheric pressure wave (TIAPW) been studied.”

- Line 83, change “(air-water-air-coupling process)” to “through air-water-air-coupling process”?

Response:

Thank you very much for your suggestion. “(air-water-air-coupling process)” is changed to “through air-water-air-coupling process”.

- Line 86, why “Double layer airglow network” since the authors mentioned “multi-layer” in Line 87?

Response:

Thank you very much for your careful comment. “double layer” is changed to “multi-layer”.

- Line 93, please add the latitude/longitude information about “Xinglong Station”.

Response:

The latitude/longitude information (40.4°N,117.6°E) is added after “Xinglong Station”.

- Line 94-95. Are all the airglow (OH, OI, 557 nm) having the same resolution as “The temporal resolution is 1 min and the spatial 95 resolution is 1 km”?

Response:

The time resolution of OH and 557 nm airglow imager is 1 minute, while the resolution of OI airglow is 2 minutes. The spatial resolution of the airglow imager at the airglow layer is not uniform. The resolutions of OH, OI 557 nm, and OI 630 nm airglow in the zenith direction are 0.27 km, 0.29 km, and 0.77 km, respectively, while in the zenith angle of 60°, the resolutions are 1.01 km (OH), 1.11 km (OI 557 nm), and 2.65 km (OI 630 nm), respectively.

- Line 95. Can you add some reference for the “standard star map”? Or some reference how the calibration works “with the help of standard star map” here.

Response:

The following reference is added to the revised manuscript.

Garcia, F. J., Taylor, M. J., and Kelley, M. C.: Two-dimensional spectral analysis of mesospheric airglow image data, *Appl. Optics*, 36(29), 7374–7385, 1997.

- Line 96, Again, some reference is needed for “removed by differential method”.

Response:

The following reference is added to the revised manuscript.

Swenson, G. R. and Mende, S. B.: OH emission and gravity waves (including a breaking wave) in all-sky imagery from Bear Lake, UT, *Geophys. Res. Lett.*, 21, 2239–2242, 1994.

- Sections 2.2, the model description is not clear at all! Do you use WACCM-X model which has been mentioned several times in the whole paper? This part just asks the readers to read two cited papers and has never mentioned the details what the conditions to be able to simulate the tsunami after HTHH. How readers know the model results robust and reliable? Can you explain why the second type of tsunami sources is better or more realistic than the first localised source? Readers can not judge it because there is no detailed information about the “Tsunami simulation model”.

Response:

Thank you very much for your comment.

We did not use the WACCM-X model in the manuscript. We only utilized the simulation results of the WACCM-X model from Liu et al. (2023).

The detailed information of the “Tsunami simulation model” is given above.

- Lines 110-111, can you describe the variables in equations 1) and 2)?

Response:

Thank you very much for your comment. The following description is added to the revised manuscript.

where x_i , k_i , c_{g_i} ($i=1,2,3$), and ω are the position vector, wavenumber vector, group velocities, and intrinsic frequency, respectively.

- Line 112. It is weird that “There is no real-time temperature data available in this study”.

Response:

This sentence is removed from the manuscript.

- Lines 112-117, I am confused why temperature is mentioned here, which should be moved after Lines 124-125.

Response:

Thank you very much for your suggestion. Lines 112-117 are moved after Lines 124-125.

- Line 123. Why use the “HWM-14” model? Is this model suitable to study the HTHH?

Response:

Thank you for your criticism and comments. Yes, you are right. The HWM wind field is an empirical model wind field that can only reflect a long-term trend, which is not suitable for event research. Therefore, we use meteor radar wind fields to replace the HWM wind fields.

- Lines 131-149 and Figure 1. The description of Figure 1 is too general. Can you make a detailed list of the airglow (which one? Lines 133-135 only mentioned OH airglow)? The figure is very hard to follow, I have to zoom it 4 times to look carefully but it is still unclear for the wave packet in each sub-figures. Therefore it is hard to judge.

Response:

Thank you for your comments.

We have made some revisions to Figure 1 to better illustrate the wave structures. In addition, we also made a video (<https://doi.org/10.5446/66190>) to present the propagation process of wave structures. The airglow image shown in Figure 3 shows that, except for the 557.0 nm radiation at Lhasa station, all other stations exhibit OH airglow radiation.

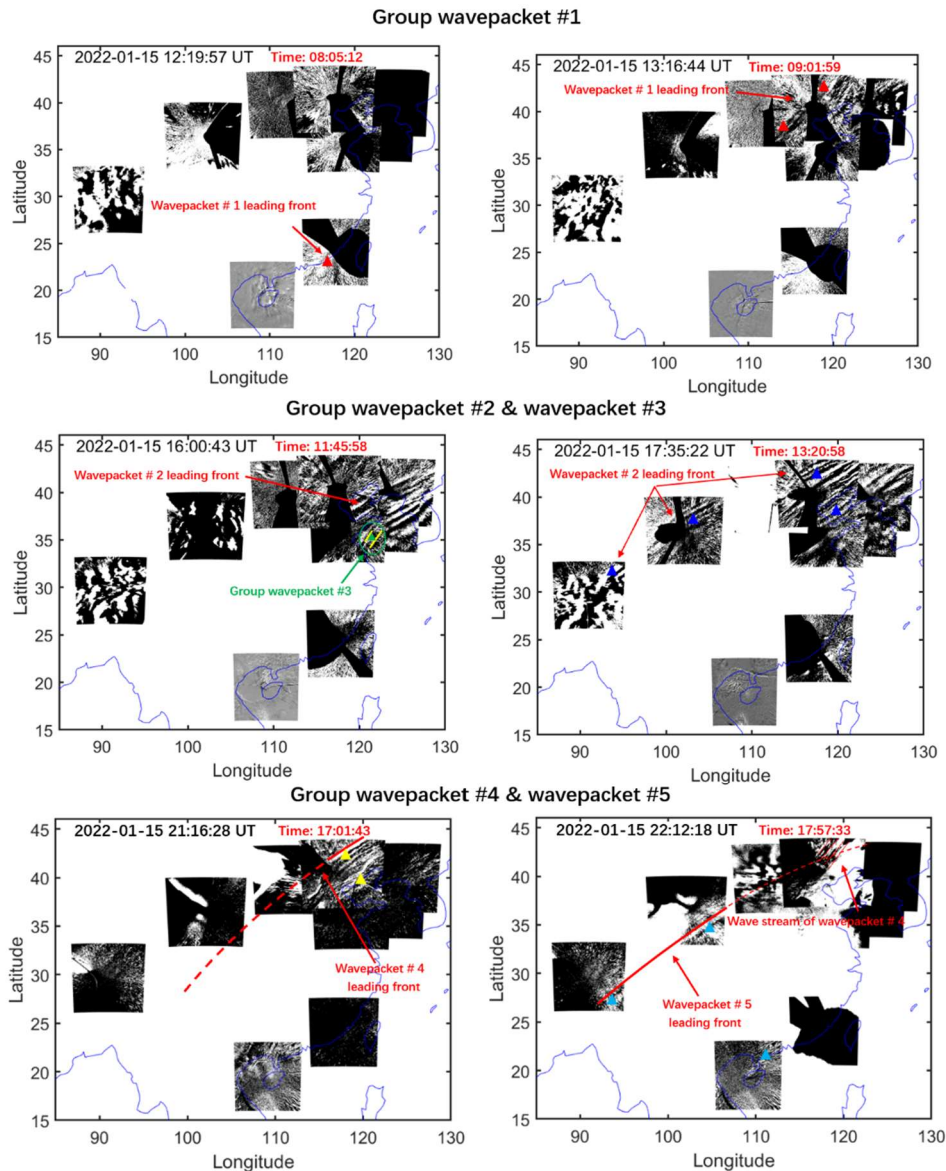


Figure 3 Five strong group atmospheric waves associated with the Tonga volcano eruptions were observed in the mesopause region by the ground-based airglow network. Different colored triangles correspond to each wave event sampling point, while red, blue, green, yellow, and cyan correspond to wave packet #1, #2, #3, #4, and #5, respectively. The red time markers in this figure and the following figure represent the lapse time since the volcano eruption.

- Line 158, It looks to me that the reference using the subscription 4 should not be the 4th reference in the list.

Response:

The correct reference is Wright et al. (2022).

- Line 159, please add some references here for the surface pressure changes.

Response:

The following reference is added to the revised manuscript.

Omira, R., Ramalho, R.S., Kim, J. et al. Global Tonga tsunami explained by a fast-moving atmospheric source. *Nature* 609, 734–740 (2022). <https://doi.org/10.1038/s41586-022-04926-4>

Takahashi, H., Figueiredo, C.A.O.B., Barros, D. et al. Ionospheric disturbances over South America related to Tonga volcanic eruption. *Earth Planets Space* 75, 92 (2023). <https://doi.org/10.1186/s40623-023-01844-1>

- Lines 159-161. It reads the logical is not clear. As mentioned Lamb wave is almost non dispersive which has purely horizontal motion. So the second sentence to Describe Figure 3 of atmospheric waves from the ionosphere to surface will cause confusion. It would be better to move or delete the first sentence.

Response:

The following sentence is removed from the revised manuscript.

Figure 3 shows vertical distribution characteristics of atmospheric waves caused by Tonga volcano eruption from the surface to the thermosphere atmosphere.

- Line 189. This is not pressure profile, it is time series of surface pressure.

Response:

“pressure profile” is changed to “time series of surface pressure”.

- Line 192, please change “position” to location.

Response:

“position” is changed to “location”.

- Lines 204-205. “are very consistent with the simulated tsunamis near the coast”? Where have you shown the simulation result?

Response:

I'm sorry, we didn't express clearly. The simulation results mentioned are shown in Figure 8 in revised manuscript.

- Line 210. Can you describe Figure 5 in detail? Just saying snapshots is not enough since the contour unit is in cm.

Response:

Thank you for your comments. We give a more detailed description as follows:

Figure 8 shows snapshots of the TIAPW and TITVE simulation results. The leading TIAPW excited by the pressure disturbances travels at the same speed as the atmospheric pressure wave and is followed by subsequent sea waves generated earlier in the atmospheric pressure wave propagation which thereafter travel at the conventional tsunami propagation speed. Under a given pressure gradient, the discharge flux in deep sea is much greater than that in shallow water. A deep bathymetric feature such as the Kermadec Tonga Trench can more effectively generate tsunami waves. The wave train following the leading wave travelling over the trench appear to be larger than those travelling in other directions. The propagation speed of TITVE from the shallow water (long) wave approximation is $v = \sqrt{gH_0}$ (Salmon, 2014), where g is the gravitational acceleration and H_0 is the ocean depth. For sea water with a general depth of 4 km, the speed of shallow water wave is about 200 m/s. Therefore, the TIAPW is significantly faster than the TITVE. The amplitude of TITVE is greater than that of tsunamis generated by atmospheric pressure waves. The wave train following the leading wave of TITVE exhibit finer structures with scales smaller than that of TIAPW. We found that the TIAPW arrived along the coast of Chinese Mainland about 4-5 hours earlier than the TITVE.

- Lines 216-218. What the evidence (where the results, assuming Figure 5 but it is vague in its description) to support these?

Response:

Thank you very much for your comments.

Air pressure waves are not very efficient at directly exciting tsunamis in shallow water due to the weaker air-sea coupling. The Yellow sea is quite shallow, so the amplitude of the leading tsunami wave directly excited by the air wave is small there and not visible using the current colormap of the plot. The waves that you can clearly see from the air-wave generated tsunami snapshots are the subsequent waves with larger amplitudes that follow the leading wave. These subsequent waves were also generated by the air-wave but when it was traveling over the deeper ocean.

- Lines 241-243. How do you estimate the wavelength? Which one (TIAPW, TITVE) or both are consistent with the derived from the airglow network which was mentioned in Lines 204-205?

Response:

Taking TIAPW as an example, we take three lines along the wave vector direction, and each line segment takes four sampling points (red points in the Figure S2 below) at the peak position. The distance between the two adjacent sampling points is the wavelength. The average wavelength can be obtained by averaging the distances between all neighboring points

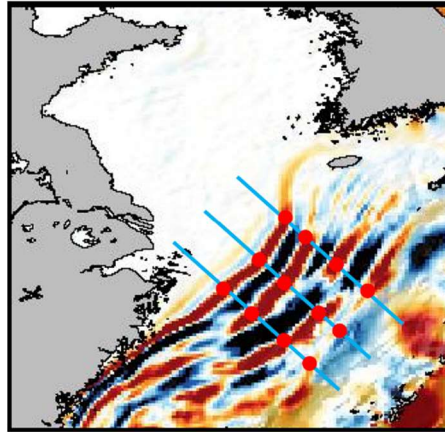


Figure S2

The average wavelength derived from TIAPW is $82 \text{ km} \pm 4\text{km}$, while the average wavelength derived from the airglow network is $84 \text{ km} \pm 5\text{km}$.

The average wavelength derived from TIAPW is $95 \text{ km} \pm 5\text{km}$, while the average wavelength derived from the airglow network is $89 \text{ km} \pm 6\text{km}$.

Therefore, compared to TITVE, the wavelength of TIAPW is more consistent with the results from the airglow network.

- Line 255-256. If wind comes from ERA5 (which has hourly product), why use SABER temperature?

Response:

Thank you for your comment. Due to the lower boundary of the SABER temperature field starting from approximately 15 km, the ERA-5 temperature field is used in areas below 15 km altitude.

- Figure 8c. Why the ray tracing calculation shows similar gradient (for example, sharp gradient around 60 km) for different sampling points A1, A2 and A3?

Response:

Due to the almost no change in the wind field at points A1, A2, and A3, meanwhile, the temperature field comes from the same SABER temperature profile, so the trajectory changes of ray tracing are almost identical

- Line 288. “If AGWs observed by the airglow network satisfy the dispersion relation” reads weird, since the figures/main text are trying to persuade the readers the current work from the multi-layer airglow observation network has detected the information of AGWs, then lines 117-118 from the reference gives the dispersion relationship of AGWs and there is a proximate relationship in Lines 279-281...

Response:

I'm sorry for not expressing clearly and causing confusion to you.

What we want to express is that the free oblique propagation characteristics of gravity waves satisfy the relationship between horizontal propagation distance and oblique propagation angle derived from dispersion relationships. We have re described as follows:

If the AGWs observed by the airglow network propagate freely rather than being constrained by duct, we will obtain the propagation characteristics similar to that observed by Azeem et al. (2007) in the ionosphere from TEC observations.

- Line 319: SWITVE should be TTIVE?

Response:

“SWITVE” is changed to “TITVE”.

- Line 334. Similar comment as above.

Response:

Thank you very much for your comment.

This aspect has been further elaborated in the main text.

- Lines 335, re-order this sentence. Better move “in the mesopause region” after AGWs?

Response:

“in the mesopause region” is moved after “AGWs”.

- Line 345, why “directly”? remove it.

Response:

“directly” is removed from the revised manuscript.

- Figure 10. Can you explain more about this possible mechanism? It is too general. It is well known how important the coupling processes among ocean/land/atmosphere to study the whole atmosphere etc.

Response:

Thank you very much for your suggestion. We give a more detailed description as follows:

The 2022 HTHH volcano eruption form a complex coupling relationship in the land-ocean-atmosphere system (Fig. 14). Firstly, the heat released by the eruption has a direct impact on the ocean, causing temperature changes in the surrounding waters. This can lead to changes in the marine environment, affecting the behavior, distribution, and ecosystem structure of organisms.

Meanwhile, volcanoes release gases such as carbon dioxide and sulfur dioxide. Carbon dioxide is one of the greenhouse gases that can cause an increase in Earth's temperature, leading to global warming. Sulfur dioxide can cause sulfuric acid mist in the atmosphere, which affects the reflectivity and temperature of the atmosphere, and thus affects the global climate.

Moreover, the 2022 HTHH volcano eruptions also trigger atmospheric waves and tsunamis. The surface atmospheric pressure wave generated by the 2022 HTHH volcano eruption can affect the upper atmosphere. The conventional tsunami triggered by the Tonga volcano generated AGWs. The atmospheric pressure wave from the eruption generated a fast tsunami never before observed by tsunami observation networks. When the tsunamis reach the coast, their speeds decrease but their amplitudes increase, and the AGWs generated by them will also affect the upper atmosphere. These AGWs play an important coupling role between the ocean and the atmosphere by affecting the density and pressure distribution of the atmosphere during propagation, leading to changes in the wind field and affecting global atmospheric circulation. This study exhibits special dynamic coupling process between air and sea via acoustic gravity waves (Fig. 14). This indirect impact on the upper atmosphere provides a new perspective for us to study the coupling between the ocean and the atmosphere and a key opportunity to improve the air-sea coupling model, thereby enhancing our future ability to make tsunami warning forecasts.

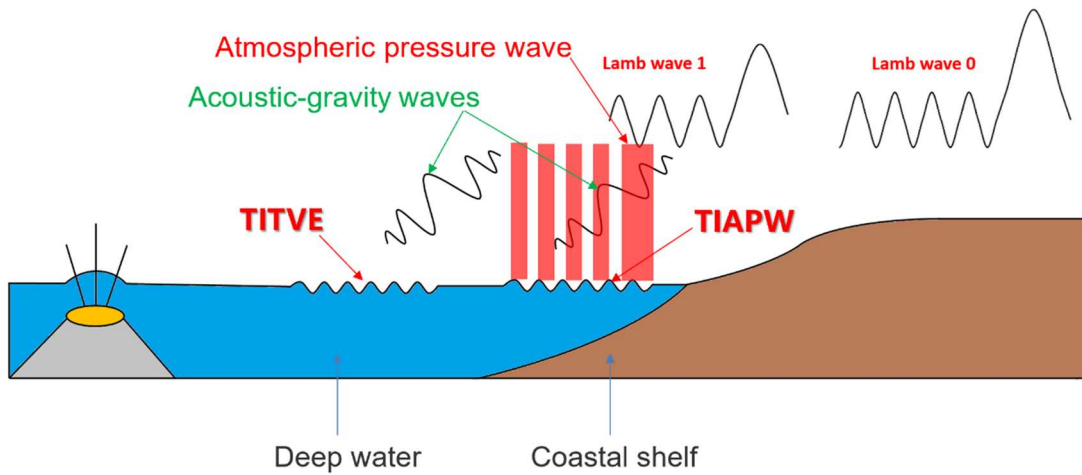


Figure 14 The Tonga volcano eruptions triggered two types of tsunamis, one type of tsunami is induced by the atmospheric pressure wave (TIAPW) and the other type tsunami is directly induced by the Tonga volcano eruption (TITVE). The acoustic gravity waves (AGWs) caused by tsunamis can propagate to the mesopause region.